ARTICLE

Near-ultraviolet Incoherent Broadband Cavity Enhanced Absorption Spectroscopy for OClO and CH$_2$O in Cl-initiated Photooxidation Experiment

Mei-li Dong[a,b], Wei-xiong Zhao[a,b], Ming-qiang Huang[c], Wei-dong Chen[d], Chang-jin Hu[a,b],

Xue-jun Gu[a,b], Shi-xin Pei[e], Wei Huang[a,b*], Wei-jun Zhang[a,b*]

a. *Key Laboratory of Atmospheric Composition and Optical Radiation, Anhui Institute of Optics and Fine Mechanics, Chinese Academy of Sciences, Hefei 230031, China*
b. *Lab of Atmospheric Physico-Chemistry, Anhui Institute of Optics and Fine Mechanics, Chinese Academy of Sciences, Hefei 230031, China*
c. *Department of Environmental Science and Engineering, Tan Kah Kee College, Xiamen University, Xiamen 363105, China*
d. *Laboratoire de Physicochimie de l'Atmosphère, Université du Littoral Côte d'Opale, 189A Av. Maurice Schumann, 59140 Dunkerque, France*
e. *School of Physics and Optoelectronic Engineering, Nanjing University of Information Science and Technology, Nanjing 210044, China*

Chlorine dioxide (OClO) is an important indicator for Cl-activation. The monitoring of OClO appears to be crucial for understanding the chemistry of Cl-initialed oxidation and its impact on air quality in polluted coastal regions and industrialized areas. We report the development of a Xe arc lamp based near-ultraviolet (335−375 nm) incoherent broadband cavity enhanced absorption spectroscopy (IBBCEAS) spectrometer for quantitative assessment of OClO in an atmospheric simulation chamber. The important intermediate compound CH$_2$O, and other key atmospheric trace species (NO$_2$) were also simultaneously measured. The instrumental performance shows a strong potential of this kind of IBBCEAS instrument for field and laboratory studies of atmospheric halogen chemistry.

Key words: Incoherent broadband cavity enhanced absorption spectroscopy, Near-ultraviolet, OClO, CH$_2$O

I. INTRODUCTION

The Cl atom, because of its high reactivity with volatile organic compounds (VOCs) as well as ozone (O$_3$), plays a significant role in the oxidative chemistry of the troposphere. For instance, the reaction rate coefficients of most alkanes with Cl-atoms is one to two orders larger than that with OH radical [1, 2]. It is demonstrated that Cl acts as an organic oxidant in coastal and industrialized areas. At dawn, Cl-initiated oxidation of VOCs is estimated to be comparable with that initiated by OH [3]. A major focus of research on the magnitude and sources of Cl atom were reported in recent years [2, 4].

Chlorine dioxide (OClO) is an important indicator for Cl-activation [5]. The monitoring of OClO appears to be crucial for understanding the chemistry of Cl-initialed oxidation and the important consequences for air quality in polluted coastal regions and industrialized areas. UV-Vis spectroscopy method is most often employed to measure OClO, such as satellite measurement [5, 6] and ground based long-path differential optical absorption spectroscopy (LP-DOAS) [7]. However, satellite measurements have a limited temporal resolution and are not sensitive for the lower troposphere [8]. In LP-DOAS measurements, long base length (between emitting and receiving units) ranging from some hundreds of meters to several kilometers are usually used to reach the necessary detection sensitivity [7] in combination with long averaging time, apart from the difficulty in optical alignment, short length-scale and short time-scale mixing ratio variation are not observable. Development of new spectroscopic technique for OClO detection with high spatial and temporal resolutions is highly desiderated for study of degradation mechanisms of atmospheric relevant organic compounds and the stratospheric ozone depletion.

In this work, we study the development of a near-UV incoherent broadband cavity enhanced absorption spectroscopy (IBBCEAS) setup based on a short arc Xe lamp source operating in the spectral range between 335
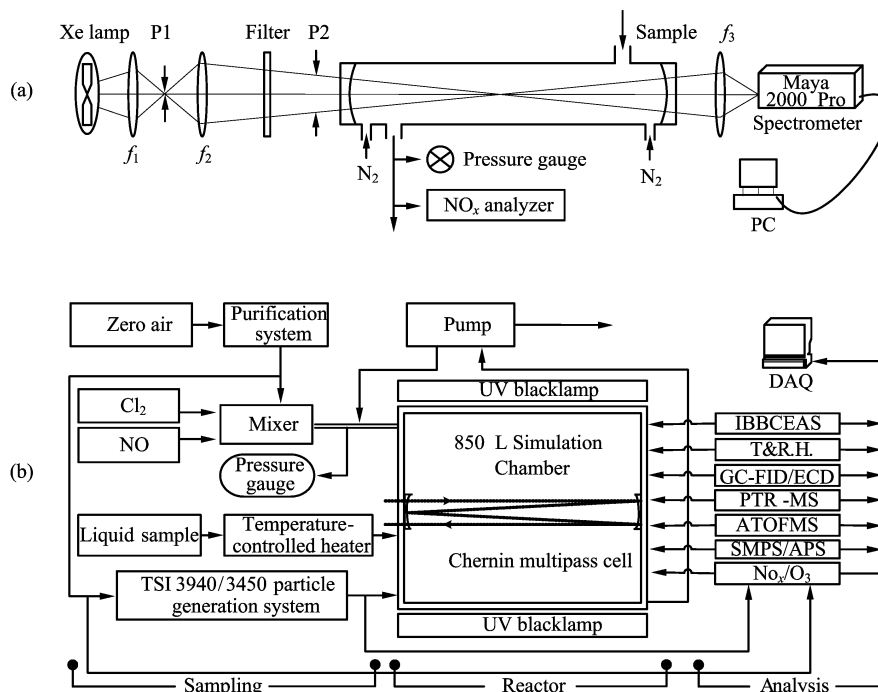
FIG. 1 (a) Schematic diagram of the Xe lamp-based incoherent broadband cavity enhanced absorption spectrometer. (b) Configuration of the used simulation chamber.

and 375 nm at room temperature. IBBCEAS based on utilization of high finesse optical cavity, firstly proposed by Fiedler *et al.* [9], has been demonstrated as a viable alternative to cavity ring down spectroscopy (CRDS) to achieve several kilometers long optical path length based on a base length of ∼1 m, which provides a useful tool for trace species concentration measurements with high spatial and temporal resolutions. Coupled with broad band light sources, such as Xe arc lamp [9, 10], light emitting diode (LED) [11, 12] or supercontinuum source [13], IBBCEAS permits for simultaneous multispecies measurements of key atmospheric trace gases, including NO_2, NO_3, N_2O_5, HONO, H_2O, O_2-O_2, O_3, I_2, IO_2, BrO, SO_2, and CHOCHO [14−16].

In the present work, quantitative assessment of OClO in a simulation chamber using IBBCEAS technique was demonstrated for the first time, to the knowledge of the authors. Formaldehyde (CH_2O), important intermediate compound in the degradation of VOCs in the troposphere, and other key atmospheric trace species (NO_2 and HONO) were also simultaneously detected. The instrumental performance of the present IBBCEAS system shows a strong potential for field and laboratory studies of atmospheric halogen chemistry.

II. EXPERIMENTS

A. IBBCEAS spectrometer

A scheme of the developed IBBCEAS setup is shown in Fig.1(a). Broadband radiation is provided by a short-

arc Xe lamp (Osram XBO 150 W/4) source with a F/1.5 single element fused silica condenser (Newport 66906). Intensity variations in the lamp output were typically <0.3% (1σ) during the measurements in the present work. Light from the incoherent Xe arc lamp passed through a telescope, which consisted of two 25 mm diameter lens (f_1=50 mm and f_2=75 mm), and focused at the centre of a high finesse optical cavity.

In order to avoid CCD detector saturation at the edges of high reflectivity range of the cavity mirrors, two band-pass filters, Schott UG11 (270−380 nm) and Semrock FF01-357/44-25 (335−380 nm), were placed between the telescope and the optical cavity to well block the lamp light radiation out of the cavity mirror's reflectivity band. The optical cavity was made of a 102 cm long quartz tube with an inner diameter of 25 mm, closed with two highly reflective mirrors (Layertec GmbH, 25 mm diameter, 1 m radius of curvature, R>99.9% between 340−370 nm). The cavity mirrors were purged with pure N_2 during experiments (0.1 L/min at each mirror). The effective optical cavity length for sample absorption was 70 cm. Gaseous sample was continuously flowed through the cavity cell at atmospheric pressure with a flow rate of 1 L/min. The stability of the pressure in the cavity, monitored by a pressure gauge, was better than 10 Pa. Light emerging from the cavity was collimated with a 25 mm diameter achromatic lens (f_3=50 mm) and then focused into a spectrograph (Ocean optics Maya 2000 Pro). The spectrograph was configured to work in the spectral range of 240.3−695.9 nm with a spectrum resolution of 0.4 nm

(using a slit width of 10 μm).

B. Atmospheric simulation chamber

The Cl atom initiated photooxidation experiment was performed by UV-irradiation of Cl_2/toluene/NO/air mixtures (initial concentrations: 2 ppmv toluene, 4 ppmv Cl_2, and 2 ppmv NO) in a 850 L sealed collapsible simulation chamber (Fig.1(b)) [17]. The chamber was made of FEP Teflon film bag, and housed inside an aluminum enclosure. The Teflon bag was surrounded by 12 fluorescent black lamps used as photolysis light and to initiate the reactions. The power of each lamp was 40 W (specified by the manufacturer) and the wavelength range of the UV radiation was 300−400 nm (measured with a CCD spectrograph). Prior to the beginning of each experiment, the chamber was continuously flushed with particle free zero air from an air purification system (Thermo 111). Temperature and humidity in the chamber were measured with a temperature and humidity sensor (Vaisala HMT333). The gas phase substances were monitored with an ozone analyzer (Thermo 49i), a NO_x analyzer (Thermo 42i) and a gas chromatograph combined with a flame ionization detector (GC-FID, Agilent 7820A). In all experiments, the relative humidity was in the range of 65%−70% at a temperature of 300±2 K.

III. SPECTROMETER CHARACTERIZATION

A. Determination of cavity mirror reflectivity

Based on the measurements of the light intensities transmitted through a high finesse optical cavity, the optical extinction coefficient $\alpha(\lambda)$ due to the sample present inside the cavity can be expressed as [16]:

$$\alpha(\lambda) = \left[\frac{1 - R(\lambda)}{d} + \alpha_{\text{Ray}}(\lambda) + \alpha_{\text{Mie}}(\lambda) \right] \cdot \left[\frac{I_0(\lambda)}{I(\lambda)} - 1 \right] \quad (1)$$

where R is the mirror reflectivity, d is the length in which the absorber is present in the cavity, $\alpha_{\text{Ray}}(\lambda)$ and $\alpha_{\text{Mie}}(\lambda)$ are the Rayleigh and Mie scattering coefficients, and $I_0(\lambda)$ and $I(\lambda)$ are the light intensities transmitted through the cavity without and with absorbing species, respectively.

For quantitative analysis, the mirror reflectivity has to be experimentally determined, which can be performed by: (i) measurement of the cavity-ring down time or phase shift [18], (ii) measurement of absorption spectrum of an absorber with known concentration and known absorption cross-section [11, 12, 19, 20], or (iii) addition of gases with different Rayleigh cross-section [16]. In the present work, the mirror reflectivity was calibrated using the 3rd method. The spectral profile

of the mirror reflectivity was deduced from the difference in the transmitted intensities of N_2 and CO_2 (or N_2 and SF_6) related to Rayleigh scattering.

The advantage of this method is that the Rayleigh extinction varies slowly with wavelength and provides a smooth mirror reflectivity spectrum over the whole working spectral region [10, 16]. The cavity was flushed with N_2, CO_2, and SF_6 at 1 L/min rate for half an hour for each species before the measurements of its scattering spectra, until the transmitted light intensity attained a stable value. The Rayleigh cross-sections used for the mirror reflectivity calculation were reported by Naus and Ubachs [21], Sneep and Ubachs [22], with an experimental uncertainty of 1% for N_2, 4% for CO_2 and 3% for SF_6. The mean uncertainty of the determined $(1-R)$ by SF_6 and CO_2 are 1.7% and 3.0%, respectively. The mirror reflectivity was found to be about 99.94%, which corresponds to an effective absorption path length of ∼1.17 km (d=70 cm).

B. Trace gases concentrations retrieval

The trace gas concentrations were retrieved using a script mode of the spectroscopic software DOASIS [23] using the following equation:

$$\alpha(\lambda) = \sum n_i \sigma_i (s_i + t_i \lambda) + P(\lambda) \quad (2)$$

where n_i is the number density and σ_i is the absorption cross-section for the ith absorber. s_i and t_i are the shift and stretch coefficients for each absorber in order to reconstruct an accurate wavelength calibration. Polynomial offset $P(\lambda)$, varying from linear to 4th order, was used to account for baseline variation due to Rayleigh and Mie scattering, and unspecified background change in the spectra related to unstable lamp emission or unstable dark current variation in the CCD spectrometer. Considering the good stability of our system, a linearly polynomial offset was used for the data retrieval.

The 2σ detection sensitivity (signal-to-noise ratio, SNR=2) was estimated by dividing the 2σ standard deviation (SD) in the broadband fitted residual spectrum of interests (in cm^{-1}) by the absorption cross-section (in cm^2/molecule) [15].

C. Performance evaluation of the spectrometer

The Rayleigh scattering method permits for determination of a smooth mirror reflectivity spectrum over the working wavelength region. However, the extinction by Rayleigh scattering is relatively small and susceptible to be perturbed by the variation of lamp intensity. In order to remedy this potential error and check the determined mirror reflectivity, absorption spectrum of O_2 dimer in pure O_2 was recorded. As O_2-O_2 dimer is stable, the absorption spectrum of O_2-O_2 can thus be used as a convenient standard reference for absolute
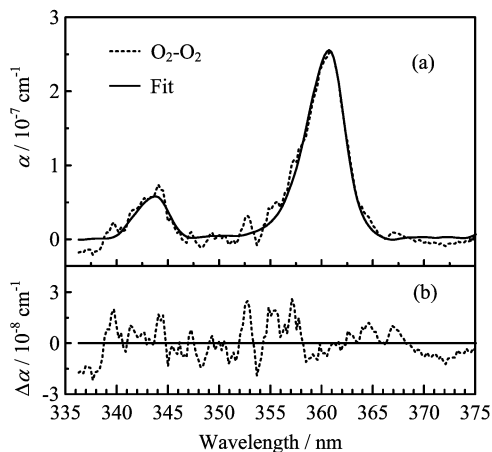
FIG. 2 (a) IBBCEAS absorption spectrum of O_2-O_2 recorded at 101 kPa. (b) Fit residual with a 1σ standard deviation of 1.0×10^{-8} cm^{-1}.

determination of the cavity mirror. The mirror reflectivity curve determined by Rayleigh scattering method was scaled to the absolute reflectivity value according to the absorption spectrum of oxygen collisional pair O_2-O_2 with known concentration. In the experiment, pure oxygen was introduced into the cavity at a flow rate of 1 L/min. Figure 2 shows an IBBCEAS spectrum of the O_2 dimer at 101 kPa between $340-370$ nm. The experimental extinction coefficient was fitted (Eq.(2)) to the reference O_2-O_2 cross section [24] using the spectroscopic software DOASIS.

The volume mixing ratio of oxygen collisional pair to oxygen of 0.988 ± 0.011, retrieved from the absorption spectrum, agreed well with the theory result, which confirmed the accuracy of the mirror reflectivity determined by the Rayleigh scattering approach. A 1σ minimal detectable extinction coefficient of 9.8×10^{-9} cm^{-1} was deduced from the standard deviation of the residuals between the measured and the fitted absorption coefficient of O_2-O_2.

In order to characterize the linearity of the system response and its detection limit, concentrations of dilution NO_2 were measured over a large range from 2 ppbv to 400 ppbv. NO_2 samples at different concentrations were generated by mixing pure NO_2 with dry N_2 to ppmv level and then further diluted with dry zero air (Thermo Zero Air Supply, Model 111) to ppbv level. Different mixing ratios were achieved by varying the flow rates of NO_2 and zero air through two mass flow controllers.

N_2 and NO_2 were continuously flowed through the cavity at atmospheric pressure with a flow rate of 1 L/min. The output flow from the cavity was split into two parts. One flow ($\sim$0.6 L/min) was directed to a commercial NO_x analyzer (Thermo 42i) for NO_2 concentration measurements, used for comparison with the result from the IBBCEAS measurements. The second flow was filtered and then pumped to outside.
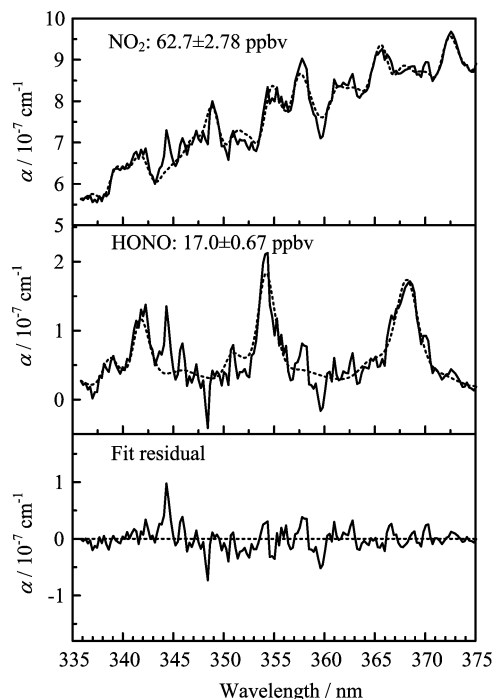
FIG. 3 Absorption spectra of NO_2 and HONO measured by IBBCEAS. The 1σ standard deviation of the residual was 2.1×10^{-8} cm^{-1}. Dotted lines are fitted absorption spectra.

For a demonstration of simultaneous measurement of NO_2 and HONO, the zero air was humidified with a Nafion tube (Perma Pure®) to form HONO by heterogeneous reaction of NO_2 with water on the surface of the experimental systems [25]:

$$2NO_2 + H_2O \xleftarrow{\ h\nu\ } HONO + HNO_3 \qquad (3)$$

Figure 3 shows a fit result of a typical IBBCEAS spectrum of HONO and NO_2 measured with a total acquisition time of 64 s (integration time: 1.6 s, spectra averaging: 40). The used cross sections of NO_2 and HONO were from Bogumil *et al.* [26] and Bongartz *et al.* [27]. As shown in Fig.3, the NO_2 and HONO concentrations retrieved from the spectrum were 62.7 ± 2.8 and 17.0 ± 0.7 ppbv (the 1σ statistical error of the spectral fit (2.8 and 0.7 ppbv) are merely a measure for the quality of the fit). The RMS of the fits of the spectra was 2.08×10^{-8} cm^{-1}, which corresponding to a 2σ detection limit of 4 and 14 ppbv for HONO and NO_2 respectively.

Figure 4 shows the result of the IBBCEAS measurements of NO_2 samples with concentrations varying from 2 ppbv to 400 ppbv, in comparison with the results obtained from the commercial NO_x analyzer. A linear relationship between two measurement results was observed over a wide range of NO_2 concentrations, with a slope of 1.005 and a R^2 value of 0.998 (Fig.4(b)).

Chin. J. Chem. Phys., Vol. 26, No. 2

Absorption Spectroscopy for OClO and CH₂O   137
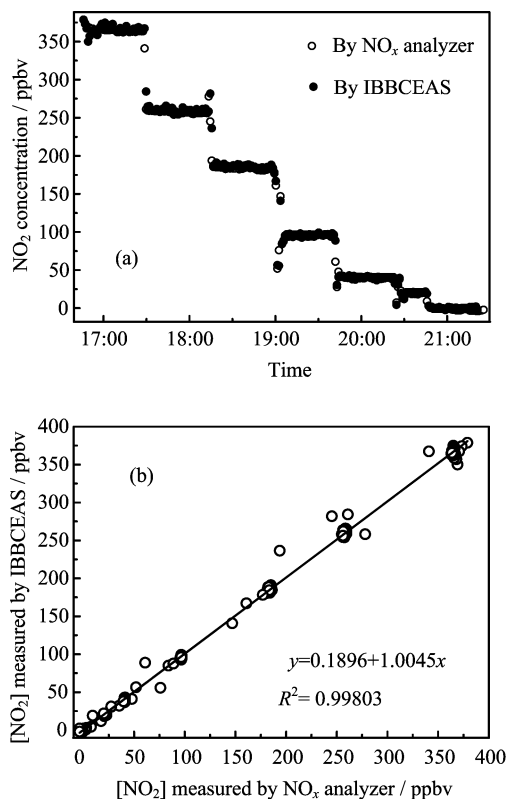
FIG. 4 (a) IBBCEAS measurements of NO₂ concentrations (ranging from 2 ppbv to 400 ppbv) in comparison with the results from a commercial NO$_x$ analyzer. (b) Correlation plot showing a linear agreement over a wide concentration range.

FIG. 5 Proposed reaction mechanism leading to the formation of OClO and CH₂O from Cl-initiated oxidation of toluene.

IV. OCLO MEASUREMENT IN AN ATMOSPHERIC SIMULATION CHAMBER

In the troposphere, toluene can be transformed by gas-phase reactions with Cl atom via H-atom abstraction reaction. As shown in Fig.5, following the initial H-atom abstraction process by Cl atoms, the oxygen molecule adds to the radical to form the benzyl peroxy radicals which can react with atomic Cl to form benzaldehyde and ClO radical. In the presence of NO, benzyl peroxy radicals may react with NO to form the corresponding alkoxy radical, oxygen can abstract a hydrogen atom from the alkoxy radical to form benzaldehyde and HO₂ radical. HO₂ radical can further react with ClO radical, leading to the formation of OClO and OH radicals. Also, benzyl alkoxy radical may crack to form benzyl radical and formaldehyde, as shown in Fig.5 [17, 28].

In the present work, OClO and CH₂O samples were produced from UV-irradiation of toluene/Cl₂/NO/air mixture in a 850 L atmospheric simulation chamber. Prior to the experiment, the chamber was continuously flushed with purified laboratory compressed air for 40 min. Toluene (C₇H₈) was injected into a 250 mL glass sampling bulb which wrapped in a temperature

controlled heater (50−300 °C). The evaporated C₇H₈ gas was then introduced into the chamber by flushed zero air. When the toluene was homogeneously mixed with air in the chamber, NO and Cl₂ were introduced into the simulation chamber. Then the chamber was filled with zero air to nearly full. Waiting for a few minutes, four black lamps were turned on to initiate the photooxidation reaction. Cl atoms will be generated by the photolysis of Cl₂ in air at wavelengths longer than 300 nm [29]:

$$Cl_2 \xrightarrow{h\nu} Cl + Cl \qquad (4)$$

A Teflon tube was connected from the chamber to the IBBCEAS setup for gas sampling. The Teflon tube was as short as possible to minimize wall loss of the sample.

The measurements of the mixtures in the photochemical reaction system with IBBCEAS were carried out according to the following procedure. (i) Measurement of a "dark" spectrum without any light source for the dark current correction of the spectrometer. (ii) Zero air was flowed through the cavity cell for the acquisition of $I_0(\lambda)$, required as reference lamp spectrum without absorbing species. (iii) Measurement of a spectrum with the absorbers in the IBBCEAS cell, required as $I(\lambda)$. The gases mixtures were sampled directly from the photoreaction chamber. (iv) Measurement of a spectrum of zero air without any absorber in the IBBCEAS cell, required as $I_0(\lambda)$, in order to monitor the drifts in the lamp reference spectrum.

Given mirror reflectivity $R(\lambda)$ was known, the absorption coefficient of the gases mixture could be deduced from Eq.(1) and Eq.(2) with $I_0(\lambda)$ and $I(\lambda)$. A typical spectral measurement of NO₂, CH₂O, and OClO are given in Fig.6. The absorber concentrations were retrieved from the measured broadband IBBCEAS spectrum via a nonlinear least square fits to the measured absorption coefficient by Eq.(2). The retrieved concentrations were 488.0±76.5, 791.0±172.0, and 4.7±0.7 ppbv for NO₂, CH₂O, and OClO, respec-
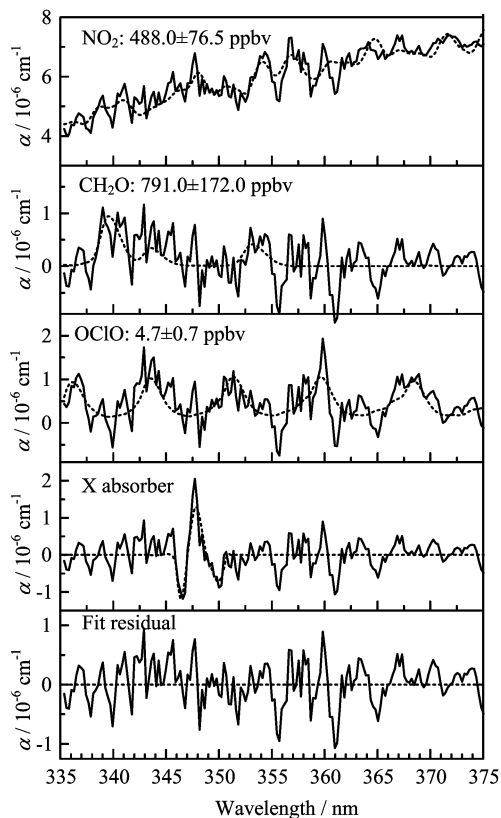
FIG. 6 IBBCEAS spectra of NO_2, CH_2O, and OClO generated using UV-irradiation of Cl_2/toluene/NO/air mixtures in a simulation chamber. The fitted residual spectrum shows a 1σ standard deviation of 3.6×10^{-7} cm^{-1}. Dotted lines are fitted absorption spectra.

tively. The cross sections of CH_2O and OClO used here were reported by Meller and Moortgat [30] and Bogumil *et al.* [26]. The 2σ standard deviation of the fit residual in Fig.6 was 7.2×10^{-7} cm^{-1}, which corresponded to a 2σ detection limit of 206 ppbv for NO_2, 524 ppbv for CH_2O, and 2.5 ppbv for OClO respectively. The absorption cross-sections used for determining the detection limit is shown in Table I.

It can be seen that the detection sensitivity is approximately 16 times lower than that obtained in particle free sample (Fig.3). This may be explained by the aerosol extinction effect [20]. A PTFE filter would be used in the future to minimize the effects of secondary organic aerosol (SOA). The photooxidation process is rather complicated, some unknown species and the unstructured absorption of SOA and the gas products, may unexpectedly contribute to the extinction in measured spectra (like X absorber exhibiting unidentifiable big absorption peak at 348 nm in Fig.6).

V. CONCLUSION

We reported the application of a near-UV IBBCEAS setup to simultaneous measurement of NO_2, CH_2O, and

TABLE I The absorption cross-sections used for determining the detection limit.

Trace gas	Absolute cross-section/(cm^2/molecule)
OClO	1.14×10^{-17}
CH_2O	5.5×10^{-20}
NO_2	1.4×10^{-19}
HONO	4.36×10^{-19}
BrO	1.3×10^{-17}

OClO in a Cl-initated photooxidation experiment in a simulation chamber. The performance of the IBBCEAS system was evaluated by simultaneous concentration measurement of NO_2 and HONO. The NO_2 measurement by IBBCEAS was compared with a commercial NO_x analyzer.

Our experiments of the first application of IBBCEAS to OClO detection show its potential for laboratory application to atmospheric halogen chemistry research. The measurement sensitivity of the present IBBCEAS system could be further improved: (i) injecting more photons into the cavity by either using a higher optical power source, efficient light coupling and an well adapted filter bandwidth, (ii) using higher reflectivity mirrors, (iii) employing high performance thermoelectric cooled CCD detector to further lower the detector noise. With further improvements, a detection sensitivity of 1×10^{-9} cm^{-1} could be achievable, which is corresponding to a 2σ detection limit of 4 ppbv of OClO.

[1] M. J. Lawler, R. Sander, L. J. Carpenter, J. D. Lee, R. von Glasow, R. Sommariva, and E. S. Saltzman, Atmos. Chem. Phys. **11**, 7617 (2011).
[2] T. P. Riedel, T. H. Bertram, T. A. Crisp, E. J. Williams, B. M. Lerner, A. Vlasenko, S. Li, J. Gilman, J. de

Gouw, D. M. Bon, N. L. Wagner, S. S. Brown, and J. A. Thornton, Environ. Sci. Technol. **46**, 10463 (2012).

[3] X. Cai and R. J. Griffin, J. Geophys. Res. **111**, 14206 (2006).

[4] J. A. Thornton, J. P. Kercher, T. P. Riedel, N. L. Wagner, J. Cozic, J. S. Holloway, W. P. Dubé, G. M. Wolfe, P. K. Quinn, A. M. Middlebrook, B. Alexander, and S. S. Brown, Nature **464**, 271 (2010).

[5] C. Tétard, D. Fussen, C. Bingen, N. Capouillez, E. Dekemper, N. Loodts, N. Mateshvili, F. Vanhellemont, E. Kyrölä, J. Tamminen, V. Sofieva, A. Hauchecorne, F. Dalaudier, J. L. Bertaux, O. Fanton d'Andon, G. Barrot, M. Guirlet, T. Fehr, and L. Saavedra, Atmos. Chem. Phys. **9**, 7857 (2009).

[6] S. Kühl, J. Pukite, T. Deutschmann, U. Platt, and T. Wagner, Adv. Space Res. **42**, 1747 (2008).

[7] D. Pöhler, L. Vogel, U. Frieß, and U. Platt, PNAS **107**, 6582 (2010).

[8] H. Kromminga, J. Orphal, P. Spietz, S. Voigt, and J. P. Burrows, J. Photochem. Photobiol. A **157**, 149 (2003).

[9] S. E. Fiedler, A. Hese, and A. A. Ruth, Chem. Phys. Lett. **371**, 284 (2003).

[10] J. Chen and D. S. Venables, Atmos. Meas. Tech. **4**, 425 (2011).

[11] S. M. Ball, J. M. Langridge, and R. L. Jones, Chem. Phys. Lett. **398**, 68 (2004).

[12] T. Gherman, D. S. Venables, S. Vaughan, J. Orphal, and A. A. Ruth, Environ. Sci. Technol. **42**, 890 (2008).

[13] J. M. Langridge, T. Laurila, R. S. Watt, R. L. Jones, C. F. Kaminski, and J. Hult, Opt. Express **16**, 10178 (2008).

[14] O. J. Kennedy, B. Ouyang, J. M. Langridge, M. J. S. Daniels, S. Bauguitte, R. Freshwater, M. W. McLeod, C. Ironmonger, J. Sendall, O. Norris, R. Nightingale, S. M. Ball, and R. L. Jones, Atmos. Meas. Tech. **4**, 1759 (2011).

[15] R. Thalman and R. Volkamer, Atmos. Meas. Tech. **3**, 1797 (2010).

[16] R. A. Washenfelder, A. O. Langford, H. Fuchs, and S. S. Brown, Atmos. Chem. Phys. **8**, 7779 (2008).

[17] M. Huang, W. Zhang, X. Gu, C. Hu, W. Zhao, Z. Wang, and L. Fang, J. Environ. Sci. **24**, 860 (2012).

[18] M. Bitter, S. M. Ball, I. M. Povey, and R. L. Jones, Atmos. Chem. Phys. **5**, 2547 (2005).

[19] I. Ventrillard-Courtillot, E. S. O'Brien, S. Kassi, G. Mejean, and D. Romanini, Appl. Phys. B **101**, 661 (2010).

[20] T. Wu, W. Chen, E. Fertein, F. Cazier, D. Dewaele, and X. Gao, Appl. Phys. B **106**, 501 (2012).

[21] H. Naus and W. Ubachs, Opt. Lett. **25**, 347 (2000).

[22] M. Sneep and W. Ubachs, J. Quant. Spectrosc. Ra **92**, 293 (2005).

[23] S. Kraus and A. Geyer, Institut fur Umweltphysik, University of Heidelberg, http://www.iup.uni-heidelberg.de/bugtracker/projects/doasis, (2001).

[24] C. Hermans, http://spectrolab.aeronomie.be/O2.htm (2011).

[25] B. J. Finlayson-Pitts, L. M. Wingen, A. L. Sumner, D. Syomin, and K. A. Ramazan, Phys. Chem. Chem. Phys. **5**, 223 (2003).

[26] K. Bogumil, J. Orphal, T. Homann, S. Voigt, P. Spietz, O. C. Fleischmann, A. Vogel, M. Hartmann, H. Kromminga, H. Bovensmann, J. Frerick, and J. P. Burrows, J. Photochem. Photobiol. A **157**, 167 (2003).

[27] A. Bongartz, J. Kames, F. Welter, and U. Schurath, J. Phys. Chem. **95**, 1076 (1991).

[28] X. Cai, L. D. Ziemba, and R. J. Griffin, Atmos. Environ. **42**, 7348 (2008).

[29] D. Maric, J. P. Burrows, R. Meller, and G. K. Moortgat, J. Photochem. Photobiol. A **70**, 205 (1993).

[30] R. Meller and G. K. Moortgat, J. Geophys. Res. D **105**, 7089 (2000).